X CONGRESSO NACIONAL DE ENGENHARIA MECÂNICA 2018
20 A 24 DE MAIO DE 2018 SALVADOR – BA – BRASIL

DEVELOPMENT OF A PROPELLER FOR AN AUTONOMOUS UNDERWATER VEHICLE WITH A HULL GEOMETRY OF THE DARPA SUBOFF MODEL

Walfrido Barnack Neto, barnack.neto@marinha.mil.br[1]
Alceu José dos Santos Moura, alceu.moura@marinha.mil.br[1]
Rubens Cavalcante da Silva, rubens.silva@marinha.mil.br[1]
Vinicius Gomes de Oliveira, vinicius.gomes@marinha.mil.br[2]
Hélio Correa da Silva Júnior, hélio.correa@marinha.mil.br[1]
Roberto Giani Pattaro Júnior, roberto.gjunior@sp_senai.br[3]
Ricardo Sbragio, sbragio@marinha.mil.br[1]

[1]Hydrodynamic Laboratory (LABHIDRO), Diretoria de Desenvolvimento Nuclear da Marinha, Av. Prof. Lineu Prestes 2468, Cidade Universitária, SP, Brazil.
[2]Centro Industrial Nuclear de ARAMAR, Estrada Sorocaba-Ipero, 12.5KM, Iperó, SP, Brazil.
[3]Faculdade de Tecnologia SENAI Roberto Mange, Rua Pastor Cícero Canuto de Lima 71, São Bernardo, Campinas, SP, Brazil.

Abstract: *This paper presents the processes of project, Computational Fluid Dynamics (CFD) simulation and manufactury of a propeller for an autonomous underwater vehicle (AUV). The AUV has a hull configuration geometrically similar to the DARPA SUBOFF model. The propeller project methodoloy uses the Liftiing Line Theory coupled with the Lifting Surface Theory in order to obtain a propeller with optimum efficiency. The analysis of the propeller operation uses CFD simulation to obtain the performance curves. Finally, the complex geometry manufacture is conducted in a CNC milling machine equiped with CAM software.*

Keywords: *Propeller, manufactury, DARPA SUBOFF, CFD simulation, Autonomous Underwater Vehicle*

1. INTRODUCTION

The Hydrodynamic Laboratory (LABHIDRO) develops a small Autonomous Underwater Vehicle (AUV) that is going to be used in the development of methodologies of identification of hydrodynamic coefficients, project methodologies and equipment tests. The hull of this AUV is geometrically similar to the DARPA SUBOFF model. The DARPA SUBOFF model was developed by the David Taylor Research Center (Bethesda, USA) and has been intensively studied and tested, which allows comparison of simulation results to test results.

One of the objectives of this AUV is to develop and compare propeller configurations. A submarine propeller shall have a high efficiency and emits low noise. The project methodologies shall be well known and tested such that the propeller fills its requirements. The first propeller version of the AUV is a conventional seven-bladed propeller projected by a combined Lifting Line Theory (LLT) and Lifting Surface Theory (LST). The propeller is adapted to the wake of the hull, which was obtained by Computational Fluid Dynamic (CFD) simulations. Its structural resistance is verified by beam theory.

The analysis of the propeller is also done in CFD simulations. The propeller performance is checked by determining the thrust coefficient (K_T) and torque coefficient (K_Q) in open water (without the AUV hull in the simulation). Future performance analysis will include CFD simulation using the entire AUV hull – propeller configuration, cavitation and performance tests in a cavitation tunnel and operational tests behind the AUV hull at sea.

The propeller is manufactured in a CNC machine center of 5 simultaneous axes. The propeller material is Aluminum AISI 6351 T6.

This article intends to describe the steps that were followed to obtain the final configuration of the propeller.

2. AUV HULL DESCRIPTION

The AUV hull is in a 1:1.588 scale of the DARPA SUBOFF model. The geometry equations of the full scale are presented by Grooves *et al*. (1989). The main dimensions are shown in the work of Toxopeus (2008) and are compared to the AUV in Tab. 1. The AUV hull is shown in Fig. 1.

Table 1. Main dimensions of the DARPA SUBOFF and of the AUV.

Dimension	Symbol	DARPA SUBOFF (Toxopeus, 2008)	AUV (1:1.588 scale)
Length Overall (m)	L	4.356	2.743
Length Between Perpendiculars (m)	L_{pp}	4.261	2.683
Maximum Hull Radius (m)	R	0.254	0.160
Volume of Displacement (m^3)	$\forall$	0.708	0.177
Wet Surface (m^2)	S	5.998	2.379

Figure 1. AUV hydrodynamic hull.

The hydrodynamic hull is divided in three parts and is manufactured in fiberglass. All equipment is installed inside the hull, in water sealed compartments.

3. METHODOLOGY

3.1. Project Methodology

The methodology used in the propeller hydrodynamic project is the circulation theory, which consists of the lifting line theory (LLT) and the lifting surface theory (LST), operating iteratively in order to obtain a propeller configuration that matches the desired thrust with an optimum efficiency. In the LLT, developed by Lerbs (1952), the blade is modeled as a lifting line with a distribution of circulation that generates the thrust. The variation of the circulation generates free vortex lines that propagate with a helical shape of constant pitch in the propeller wake. The circulation of the wake generates induced velocities on the blade, altering the inflow and the blade pitch. The results obtained from the LLT are the optimum distribution of circulation, the blade pitch angle and the induced velocities, which are the input data for the LST.

The LST was developed by Kerwin (1973). It uses the data from the LLT and is a more precise method for calculating the thrust, as it discretizes the blade radially and angularly. The initial blade pitch angle, circulation distribution and induced velocities from the results of the LLT are used as input data. In the blade surface grid, a suitable distribution of spanwise vortices, trailing vortices and sources (used to simulate thickness) determines the flow field and the final blade pitch in an iterative way. By integrating the pressure over the blade, the thrust generated by the propeller is obtained.

Differently from the propellers projected by systematic series, which are obtained by open water tests and a mean value of the wake field, the use of the circulation theory allows the propeller to be wake adapted, as it considers the radial distribution of the axial wake generated by the hull. The axial wake data was obtained by modeling the complete hull in the CFD code ANSYS CFX. The advantage of a wake adapted propeller is that the pressure distribution over the blade is more adequate, avoiding large angles of attack which could induce cavitation, separation or loss of performance.

The project methodology allows to obtain the propeller geometry and performance data only in the project point. The main objective is to maximize the propulsive efficiency, which combines the hull efficiency (e_h) and the propeller efficiency (e_p), being defined by Eq. (1).

$$\eta = e_h e_p \tag{1}$$

The hull efficiency is the relation between the power demanded by a towed hull and the power demanded by a self-propelled hull, to achieve a certain velocity, and depends on the wake coefficient and on the thrust reduction coefficient. The propeller efficiency is the relation between the power generated by the propeller and the power delivered to the propeller.

All data used in the project of the propeller are from the full model geometry, which simplifies the comparison with literature data when possible. In the fabrication phase, the propeller is scaled for the AUV dimensions. As the Reynolds numbers are close (2.23E7 for the full scale and 1.12E7 for the model), differences in frictional resistances are small.

3.2. Performance Analysis Methodology

The performance analysis of the propeller determines its open water curves by CFD calculations and/or by cavitation tunnel tests. The coefficients used in the analysis are the thrust coefficient (K_T), torque coefficient (K_Q), advance coefficient (J) and the propeller efficiency (e_p), given by Eq. (2) to (5), respectively.

$$K_T = \frac{T}{\rho n^2 D^4} \tag{2}$$

$$K_Q = \frac{Q}{\rho n^2 D^5} \tag{3}$$

$$J = \frac{V_a}{nD} \tag{4}$$

$$e_p = \frac{TV_a}{2\pi Qn} = \frac{K_T}{2\pi K_Q} J \tag{5}$$

where T is the propeller thrust, Q is the torque, ρ is the density of water, n is the rotation in [rps], D is the propeller diameter, V_a is the advance velocity (which is the AUV velocity altered by the wake coefficient).

4. RESULTS

4.1. Wake Determination

For a wake adapted propeller project, the correct determination of the wake is essential, as its velocities influence the pitch angle of the blades and the resulting forces. The wake generated by the model on the propeller plane can be evaluated either by tests or by CFD simulation.

For the case of bare hull, the wake velocity distribution is calculated using the CFD solver Ansys CFX version 17.1, and compared to the wake velocities presented in the work of Gorsky *et al*. (1990). These authors calculated the DARPA SUBOFF model wake using a Reynolds-Averaged Navier-Stokes (RANS) flow solver, which is described in their work and in its references.

The turbulence model used in the CFD simulation was the k-ω SST (Menter's Shear Stress Transport). The SST model is a combination of two of the most commonly-used two-equation models: the k-ω model in the viscous sublayer and logarithmic part and the k-ε model in the wake region of the boundary layer with a blending function that gradually switches between the models. The k-ω SST model combines the best properties of both models and therefore is an adequate choice of turbulence model for many engineering applications.

In the simulations, a cylindrical domain is used extending 6 model lengths in downstream, 4 lengths in upstream and 2.3 in radial direction. On the inlet surface a uniform inflow is set. On the outlet surface an outflow boundary condition is specified, in which the gradient in normal direction is set to zero for all flow variables. On the outer boundary a free slip wall is prescribed. On the model surface a no-slip condition is used with zero velocity. Initial and inflow turbulence quantities conditions are set to 5% turbulence. Figure 2 presents the non-dimensional velocity profile in the symmetry plane, where it is possible to notice the influence of the hull in the flow.

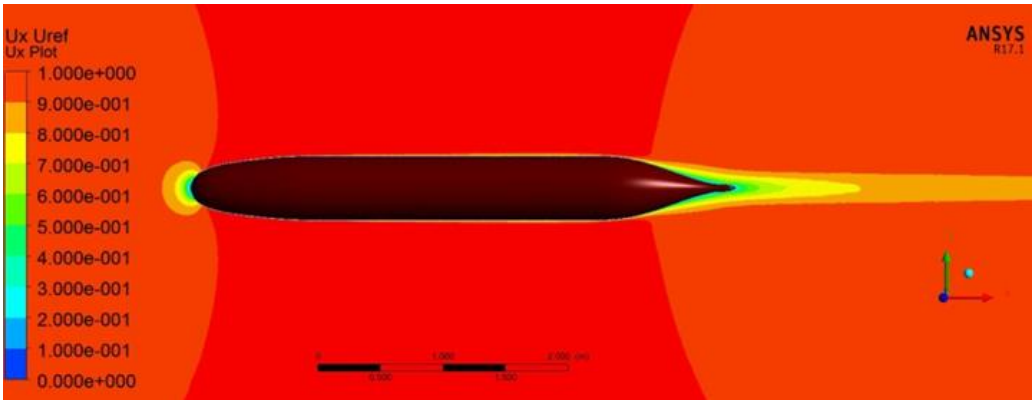

Figure 2. Non-dimensional axial flow velocity around the DARPA SUBOFF model (CFD simulation).

Gorski *et al.* (1990) present the bare hull non-dimensional axial, tangential and radial wake distributions as a function of the distance $r - r_o$, where r is the radial position and r_o is the hub radius. The data from the authors are plotted in Fig. 3 together with the CFD simulation results for the axial wake velocities at the same position (97.8% of the length). The results are considered quite adherent. The mean value of the axial wake in the propeller disk non-dimensionalized by the maximum velocity is $V_a/V_S = 0.7148$.

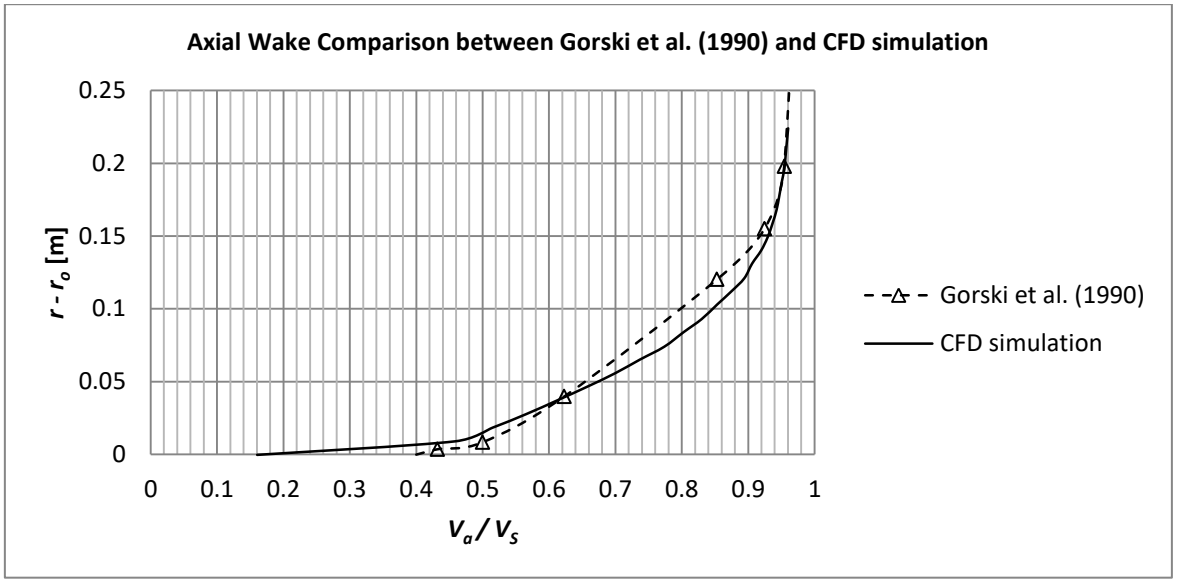

Figure 3. Comparison between the CFD axial wake results and the axial wake presented in Gorski *et al.* (1990).

4.2. Project

The propeller is projected for the full scale DARPA SUBOFF model and manufactured according to the AUV scale. The main parameters of the propeller project are described next.

4.2.1. Velocity

The velocity of the model used in the project of the propeller is the maximum velocity of 10 knots (5.14 m/s). This speed is one of the speeds at which the model was tested in towing tank, according to Liu *et al*. (1998) and is considered adequate for future maneuvering tests of the AUV.

4.2.2. Rotation Speed

The propeller maximum rotation speed is 800 rpm, for reaching the maximum velocity. This rotation was optimized for the propeller diameter, in order to reach maximum propulsive efficiency.

4.2.3. Diameter

The full scale propeller has a diameter of 0.300 m, which corresponds to 59% of the maximum hull diameter. The diameter of the hub is 20% of the propeller diameter, being equal to 0.06m.

4.2.4. Bare Hull Total Resistance

The total resistance (R_t) of the DARPA SUBOFF for a bare hull (without appendices) is divided in two parts, the viscous resistance (R_v) and the wave making resistance (R_w) and is expressed by Eq. (6).

$$R_t = R_v + R_w \tag{6}$$

These resistances are expressed in non-dimensional format by Eqs. (7) to (9):

$$C_t = \frac{R_t}{0.5\rho S V^2} \tag{7}$$

$$C_v = \frac{R_v}{0.5\rho S V^2} \tag{8}$$

$$C_w = \frac{R_w}{0.5\rho S V^2} \tag{9}$$

where C_t is the total resistance coefficient, C_v is the viscous resistance coefficient, C_w is the wave making resistance coefficient, ρ is the water density, S is the wet surface of the model and V is the velocity. Equation (6) can be expressed in non-dimensional format as:

$$C_t = C_v + C_w \tag{10}$$

The viscous resistance coefficient is estimated as being the frictional resistance coefficient of a flat plate (C_{fo}) with the same wet surface and same length of the model, altered by a form factor (k), as in Eq. (11).

$$C_v = C_{fo}(1 + k) \tag{11}$$

For the model operating totally submerged in a sufficient depth to avoid wave making, the wave making resistance is negligible and the total resistance coefficient is given by Eq. (12).

$$C_t = C_{fo}(1 + k) \tag{12}$$

The determination of the total resistance is presented next for the maximum velocity (V_s) of 10 knots and for the DARPA SUBOFF data shown in Tab. 1. The fluid density (ρ) for fresh water at 20°C is 998.2072 kg/m^3 and the kinematic viscosity (ν) is 1.0034E-6 m^2/s (ITTC, 2011).

a) Determination of the Reynolds Number (Re): the Reynolds number for the full scale model is given by Equation (13).

$$Re = \frac{V_s L}{\nu} = 2.23\text{E}7 \tag{13}$$

b) Determination of the frictional coefficient (C_{fo}): the frictional coefficient is determined from the Schoenherr line formula (Carlton, 2007) representing the model by a flat plate with the same length and wet surface, according to Eq. (14)

$$\frac{0.242}{\sqrt{C_{fo}}} = log_{10}(Re.C_{fo}); \quad C_{fo} \approx 0.002582 \tag{14}$$

c) Determination of the form factor (k): the form factor is estimated as $k = 0.195$, being a typical value for a slender body.

d) Determination of the total resistance coefficient: according to Eq. (12), Eq. (14) and the form factor value, the total resistance coefficient is given by Eq. (15):

$$C_t = C_{fo}(1 + k) = 0.003085 \tag{15}$$

e) Determination of the total resistance: the total resistance is obtained from Eq. (7) and is expressed by Eq. (16).

$$R_t = C_t \frac{1}{2}\rho S V_s^2 = 244.5N \tag{16}$$

The result of total resistance shown in Eq. (16) matches the result presented by Liu et al (1998) obtained in the tests conducted in the towing tank of the Naval Surface Warfare Center Carderock Division (NSWCCD) for the DARPA SUBOFF bare hull. In the towing test, the total resistance presented by the authors is 242.2N for the velocity of 10 knots.

4.2.5. Propeller Thrust

When positioned behind the hull, the propeller induces a pressure drop that increases the resistance. Hence, the power needed for reaching the velocity is greater than the total resistance estimated for the bare hull. The thrust

reduction factor (t) relates the bare hull resistance and the necessary thrust, according to Eq. (17). For the DARPA SUBOFF model, the thrust reduction factor is estimated as 0.20, based on hulls of similar geometry.

$$T = \frac{R_t}{1-t} = 305.6N = 31.1kgf \tag{17}$$

4.2.6. Number of Blades

The number of blades is chosen, associated with the skew angle, in order to minimize the vibration introduced in the shaft. The use of a large number of blades is desirable concerning vibration, as the intensity of the harmonics of the wake reduces. However, it becomes more difficult to manufacture the propeller due to the superposition of the blades. Due to the hull and rudders configuration (the DARPA SUBOFF uses four rudders), it is desirable to use an odd or a prime number of blades, avoiding the simultaneous angular coincidence of more than one blade with the rudder position during the propeller rotation. Hence, a number of seven blades was chosen, which is viable to manufacture and reduces the vibration in a suitable way.

4.2.7. Thickness Distribution and Section Camber

The section thickness follows a Modified NACA 66 distribution (Brockett, 1966), commonly used in propellers due to its adequate pressure distribution. The camber, or blade section mean line (ITTC, 2008), is a NACA a = 0.8 camberline, which induces a uniform chordwise loading in 80% of the section chord (starting from the leading edge) and a linear decrease through the others 20% until the trailing edge. The NACA a = 0.8 camberline is commonly used with the NACA 6-series wing sections, like the NACA 66 (Abbott *et al*., 1959).

4.2.8. Skew Distribution

The skew consists in the displacement of the blade section along the pitch helix (ITTC, 2008), as shown in Fig. 4. The skew angle distribution $\delta_S(r)$ is used to reduce propeller vibrations, together with the number of blades. In the case of a submersible, the skew is very effective in avoiding the simultaneous effect of the water blockage from the rudders over one blade during the propeller rotation. By applying a skew distribution, the blockage occurs only in one section of the blade at a time, reducing the vibration intensity.

The skew distribution used in the propeller uses a quadratic equation with 20° of skew angle in the propeller tip (where radial position r equals the propeller radius R) and -60° of derivative of the skew angle with respect to the non-dimensional radial position x, in the hub (where radial position r equals 0.2 R for this propeller).

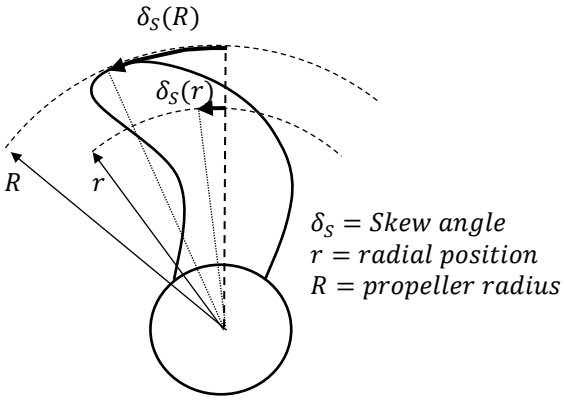

Figure 4. Skew angle.

4.2.9. Circulation Distribution

The blades are projected using the optimum distribution of circulation (Lerbs, 1952). This condition imposes that the efficiency is constant along all radial sections of the propeller blades. The use of the optimum distribution of circulation can induce strong tip or hub vortices, which is a concern for naval submarines, due to radiated noise. In the case of the DARPA SUBOFF, the intention of using the optimum distribution of circulation is to be a basis for future development of propellers and for noise and efficiency comparisons.

4.2.10. Project Main Results

The main results obtained from the propeller project are presented in Tab. 2, while the propeller design drawing is shown in Fig. 5.

Table 2. Main results.

J = Advance coefficient, Eq. (4)	0.919
V_S = Maximum velocity (knots)	10
n = Maximum rotation (rpm)	800
T = Thrust (N)	305.4
Q = Torque (Nm)	19.34
K_T = Thrust coefficient, Eq. (2)	0.2125
K_Q = Torque coefficient , Eq. (3)	0.0449
$1-t$	0.8000
$1-w$	0.7148
e_p = Propeller efficiency, Eq. (5)	0.693
e_h = Hull efficiency = $(1-t)/(1-w)$	1.119
e_t = Transmission efficiency (assumed)	0.99
η =Propulsive coeficient, Eq. (1)	0.776
$EHP = R_t * V_s$ (Effective Horse Power) (W)	1256.8
$THP = T * V_a = EHP/e_h$ (Thrust Horse Power) (W)	1123.0
$DHP = 2\pi Qn$ (Delivered Horse Power) (W)	1620.3
$BHP = DHP/e_t$ (Brake Horse Power) (W)	1636.7
Ae/Ao = Expanded Area / Disk Area	0.60374

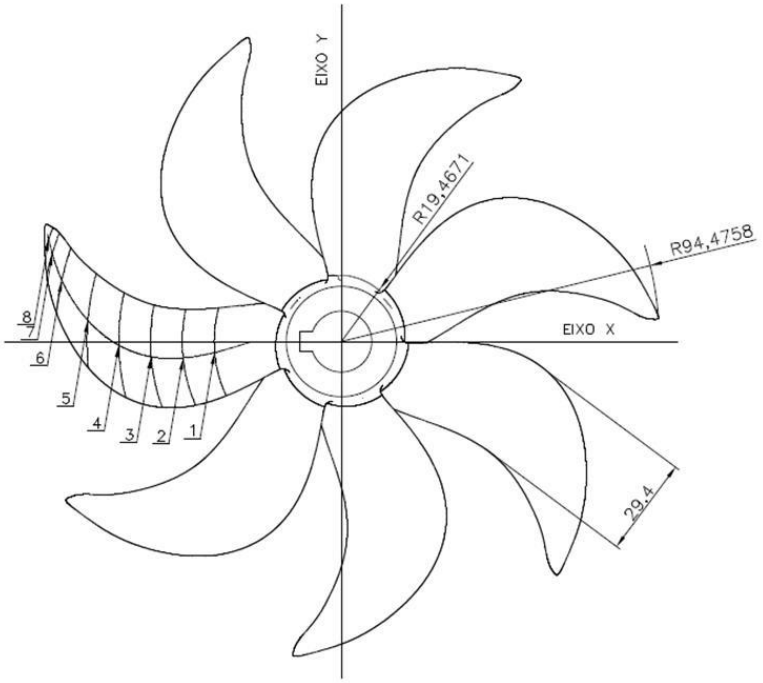

Figure 5. Seven-bladed propeller drawing with dimensional control points.

4.3. CFD Performance Analysis in Open Water

For the open water CFD simulations, a cylindrical domain of five diameters is chosen in each direction with respect to the propeller origin. At the inlet a uniform velocity is specified together with a low turbulence level. At the outlet, a relative pressure boundary condition equal to zero is used. On the outer boundary, a free slip wall is prescribed again and in the propeller blades and shaft, a no-slip condition is used. Figure 6 shows the fluid rotating domain and the element distribution at the propeller surface.

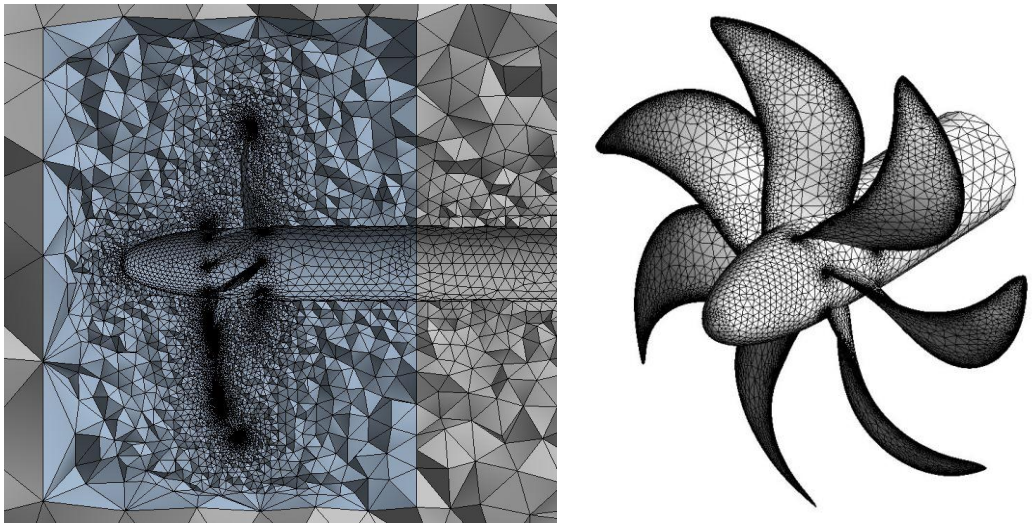

Figure 6. Views of the fluid rotating domain and the element distribution over the propeller surface.

The advance coefficient (Eq. 4) simulation range was from 0 to 1.3. The rotation rate was kept constant while the inflow velocity was varied.

Figure 7 presents the open-water diagram obtained with CFD simulations and compares the results to the project operation point values.

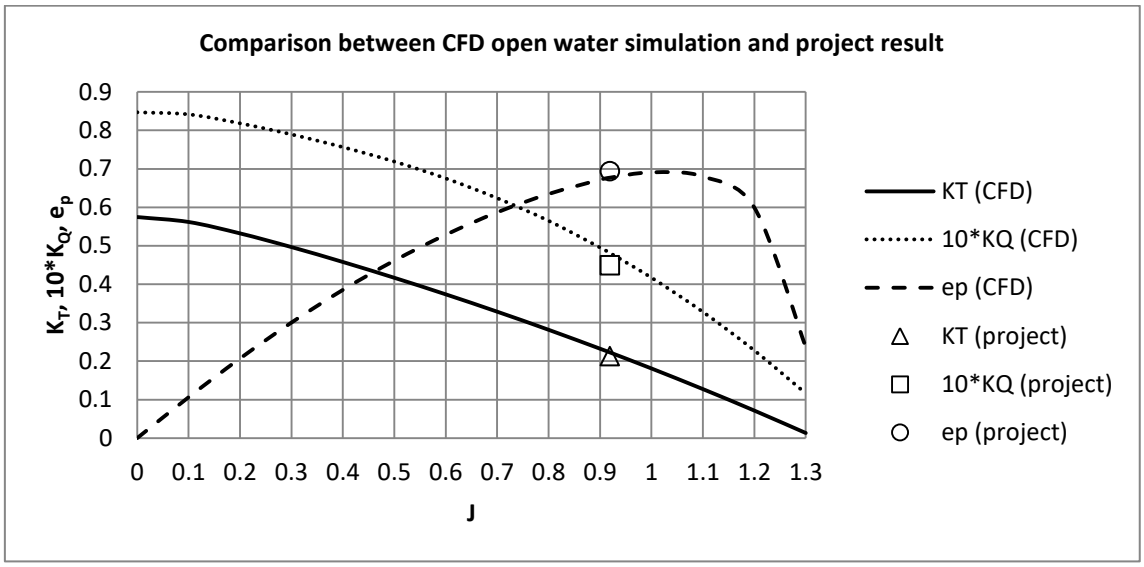

Figure 7. Comparison between CFD open water simulation and project operation point.

4.4. Structural Analysis

The structural analysis is based in beam theory. The maximum Von Mises stresses for the propeller is determined for two conditions: maximum velocity forward condition and bollard pull condition (zero velocity and maximum rotation). The material is Aluminum AISI 6351 T6 with yield strength of 65MPa. The safety factor of the propeller is 5.3 for maximum velocity condition and 2.6 for bollard pull condition. These values are considered adequate for the AUV operation.

4.5. Manufacture

The propeller manufacture was carried out at the workshops of Faculdade SENAI "Roberto Mange" (Campinas, SP) using a 5-axis machining center Hardinge XR600 5AX with PowerMill CAM software. The roughing process strategy used three simultaneous axis (X, Y and Z). The finishing process strategy used five simultaneous axis (X, Y, Z, A and C) with rotation, tilt and lead angle variation of the machining center. Both processes used ball-end cutting tools with 6mm and 3mm of diameter and 100mm total length. Cutting parameters were followed as indicated by the supplier (KENNAMETAL) to N class aluminum alloy: ap=1.5D máx, ae=0.25D máx, Vc= 250 – 750 m/min and fz= 0.024 –

0.048 mm of the machining center table. The software simulations of these processes are shown in Figs. 8 and 9 respectively. Figure 10 presents the manufactured propeller.

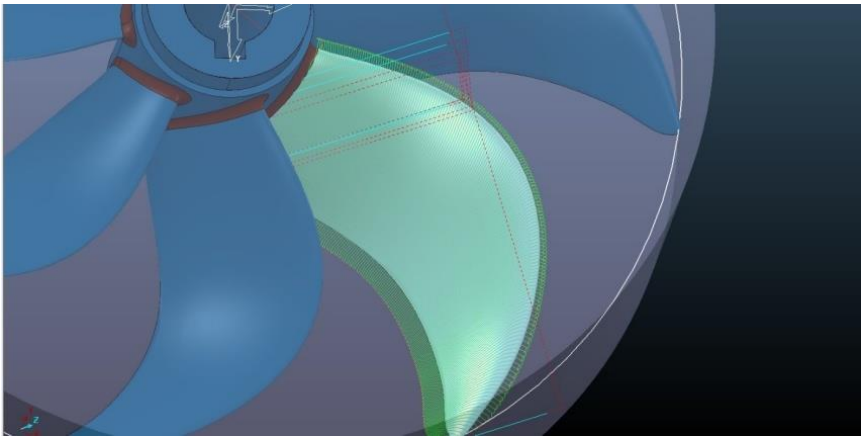

Figure 8. CAM Simulation of roughing operation.

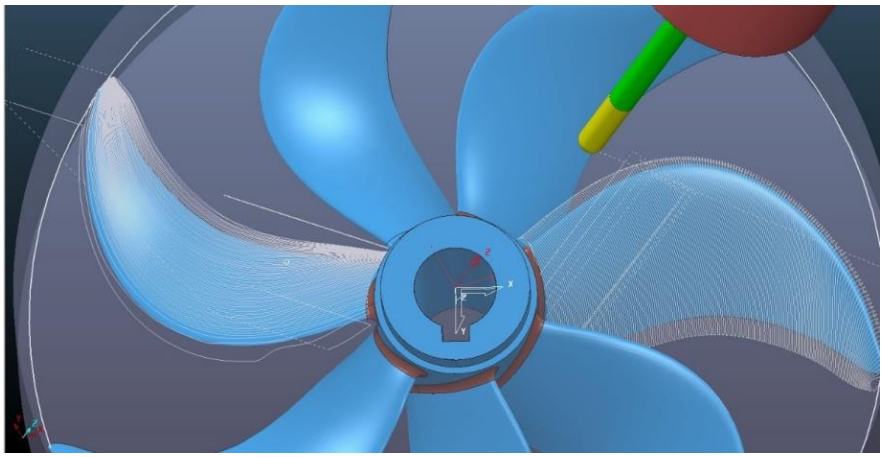

Figure 9. CAM Simulation of finishing operation.

Figure 10. Manufactured propeller.

5. CONCLUSION

The seven-bladed propeller for the DARPA SUBOFF submarine model is projected for a maximum velocity of 10 knots at a rotation of 800 rpm. It has a quadratic distribution of skew with tip angle of 20^o and -60^o of derivative with respect to the non-dimensional radius at the hub. The axial wake used in the project was determined by CFD simulations.

The hydrodynamic project uses Lifting Line and Lifting Surfaces Theories, with an optimum distribution of circulation in order to obtain maximum efficiency.

The structural analysis used beam theory in two operating conditions: maximum velocity and bollard pull conditions. The minimum safety factor is 2.6.

The propeller is manufactured in a 1:1.588 scale and will propel an AUV which is geometrically similar to the DARPA SUBOFF model. The manufacture was carried out in a 5-axis milling machining center.

The next steps in the development of this propeller are the CFD simulation using the entire AUV hull – propeller configuration, the cavitation and performance tests to be conducted in a cavitation tunnel and the operational tests aft the AUV hull at sea.

6. ACKNOWLEDGEMENTS

The authors would like to thank the Diretoria de Desenvolvimento Nuclear da Marinha, the Centro Tecnológico da Marinha em São Paulo, the Centro Industrial Nuclear de Aramar and the Faculdade de Tecnologia SENAI Roberto Mange for the support in the realization of this work.

7. REFERENCES

Abbott, I.H., Von Doenhoff, A.E., 1959, “Theory of Wing Sections”, Dover Publications, Inc., 693p.

Brockett, T., 1966, “Minimum Pressure Envelopes for Modified NACA-66 Sections with NACA a = 0.8 Camber and BUSHIPS Type I and II Sections”, David Taylor Model Bsin, Washington, DC, USA, 36p.

Carlton, J.S., 2007, “Marine Propellers and Propulsion”, 2nd Ed., Elsevier Ltd., 533p.

Gorsky, J.J, Coleman, R.M , Haussling, H.J., 1990, “Computation of Incompressible Flow Around the DARPA SUBOFF Bodies”, DTRC-90/016, David Taylor Research Center, Bethesda, MD, USA, 80p.

Grooves, N.C., Huang, T.T., and Chang, M.S., 1989, “Geometric Characteristics of the DARPA SUBOFF Models (DTRC Models No. 5470 and 5471)”, DTRC/SHD-1298-01, David Taylor Research Center, Bethesda, MD, USA, 75p.

ITTC, 2008, “International Towing Tank Conference Recommended Procedures – Model Manufacture, Propeller Models, Terminology and Nomenclature for Propeller Geometry”, Procedure 7.5-01-02-01, Revision 01, 20p.

ITTC, 2011, “International Towing Tank Conference Recommended Procedures – Fresh Water and Seawater Properties”, Procedure 7.5-02-01-03, Revision 02, 46p.

Kerwin, J.E., 1973, “Computer Techniques for Propeller Blade Section Design”, International Shipbuilding Progress, Vol. 20, No. 227, pp. 227-251.

Lerbs, H.W., 1952, “Moderately Loaded Propellers with a Finite Number of Blades and an Arbitrary Distribution of Circulation”, Transactions of the SNAME, Vol. 60, pp. 73-123.

Liu, H.L., Huang, T.T., 1998, “Summary of DARPA Suboff Experimental Program Data”, CRDKNSWC/HD-1298-11, Naval Surface Warfare Center Carderock Division (NSWCCD), 24p.

Toxopeus, S., 2008, “Viscous-Flow Calculations for Bare Hull DARPA SUBOFF Submarine at Incidence”, International Shipbuilding Progress, Vol. 55, No. 3, pp. 227-251.

8. AUTHORAL RESPONSIBILITY

“The authors are solely responsible for the content of this article”.